LETTERS

Visualizing and controlling vibrational wave packets of single molecules

Daan Brinks[1], Fernando D. Stefani[1]†, Florian Kulzer[1], Richard Hildner[1], Tim H. Taminiau[1], Yuri Avlasevich[2], Klaus Müllen[2] & Niek F. van Hulst[1,3]

The active steering of the pathways taken by chemical reactions and the optimization of energy conversion processes[1–3] provide striking examples of the coherent control of quantum interference through the use of shaped laser pulses. Experimentally, coherence is usually established by synchronizing a subset of molecules in an ensemble[4–7] with ultra-short laser pulses[8]. But in complex systems where even chemically identical molecules exist with different conformations and in diverse environments, the synchronized subset will have an intrinsic inhomogeneity that limits the degree of coherent control that can be achieved. A natural—and, indeed, the ultimate—solution to overcoming intrinsic inhomogeneities is the investigation of the behaviour of one molecule at a time. The single-molecule approach[9,10] has provided useful insights into phenomena as diverse as biomolecular interactions[11–13], cellular processes[14] and the dynamics of supercooled liquids[15] and conjugated polymers[16]. Coherent state preparation of single molecules has so far been restricted to cryogenic conditions[17], whereas at room temperature only incoherent vibrational relaxation pathways have been probed[18]. Here we report the observation and manipulation of vibrational wave-packet interference in individual molecules at ambient conditions. We show that adapting the time and phase distribution of the optical excitation field to the dynamics of each molecule results in a high degree of control, and expect that the approach can be extended to achieve single-molecule coherent control in other complex inhomogeneous systems.

For few-atom molecules, coherent control schemes can be designed on the basis of theory[19]. For more complex systems, such as large (bio-)molecules at ambient conditions, *ab initio* quantum mechanical calculations fail, and the elegant approach of closed-loop adaptive feedback[20] has gained attention. The implementation of pulse shaping by self-learning algorithms has led to the coherent control of a wide variety of photo-induced processes: selective fragmentation[21], bond dissociation and rearrangement[22], laser-induced fluorescence[23], coherent anti-Stokes Raman[24] and high-harmonic generation[25]. In all of these studies, the time, phase and frequency content of the optical field is experimentally optimized to obtain a certain product state. The resulting optimized pulse reflects the dynamics of the underlying processes and can take non-trivial shapes.

In a single-molecule measurement, the challenge is to extract information from the limited number of fluorescence photons obtainable before photobleaching; a long optimization process is not feasible. Fortunately, optimal control theory on model systems[26,27] and experiments on large molecules[4] have demonstrated that complex pulses can often be simplified to a physically more intuitive shape with comparable efficiency. Typically, in the time domain, the optimum optical field takes the shape of a sequence of pulses separated by a time

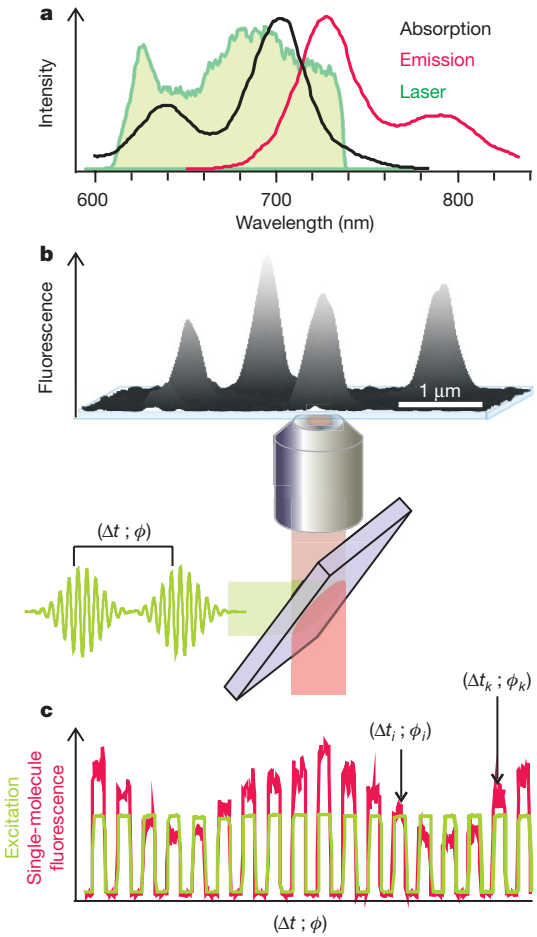

Figure 1 | Ultrafast coherent excitation of single molecules. a, Spectra of the fluorophore (DNQDI[29]; dissolved in toluene) and broad-band excitation laser used (see Methods). **b**, Single fluorescent molecules were imaged and investigated in an epi-confocal microscope. Each individual molecule was excited with tailored sequences of 15-fs (full-width at half-maximum) pulses defined by the inter-pulse time delay Δt and phase shift ϕ. Both Δt and ϕ were controlled with a double-pass 4f pulse shaper based on a spatial light modulator. **c**, The fluorescence intensity of the single molecules was recorded for different combinations of Δt and ϕ (for example, $(\Delta t_i, \phi_i)$, $(\Delta t_k, \phi_k)$, and so on), which were applied sequentially, separated by periods of no illumination and repeated until the molecule photobleached.

[1]ICFO—Institut de Ciencies Fotoniques, Mediterranean Technology Park, 08860 Castelldefels (Barcelona), Spain. [2]Max Planck Institute for Polymer Research, Ackermannweg 10, D-55128 Mainz, Germany. [3]ICREA—Institució Catalana de Recerca i Estudis Avançats, 08015 Barcelona, Spain. †Present address: Departamento de Física & Instituto de Física de Buenos Aires (IFIBA, CONICET), Universidad de Buenos Aires, Pab. I Ciudad Universitaria, 1428 Buenos Aires, Argentina.

(femtoseconds to picoseconds) that is characteristic of the molecular dynamics. We therefore interrogated the coherent dynamics of individual molecules by monitoring the fluorescence emission after excitation with a sequence of equi-spaced phase-locked laser pulses. Both the inter-pulse time delay (Δt) and phase shift (ϕ) were controlled (Fig. 1). The excitation intensity was kept constant for all (Δt, ϕ) combinations, at values causing no significant depletion of ground state population probability, so that the single-molecule fluorescence intensity provided a direct measure of the excitation probability.

In a first experiment, single fluorescent molecules were imaged under excitation with a two-pulse sequence. Each image was acquired with a particular Δt and fixed $\phi = 0$ (Fig. 2a). Even though the same excitation intensity was used for all images, the molecules fluoresce with varying intensity, depending on Δt. Remarkably, the individual molecules do not collectively appear brighter or dimmer but show characteristic individual changes in fluorescence as a function of Δt. Plotting the integrated fluorescence emission of each molecule versus Δt reveals an oscillatory behaviour of the excitation probability, as in the examples shown in Fig. 2b. Evidently, the probability of photoexcitation of the single molecules depends on the femtosecond temporal distribution of the photons available for absorption and varies from molecule to molecule.

The observed oscillatory behaviour can be explained in terms of wave-packet interference (WPI)[28]. Initially, the molecule is in the electronic ground state. The first optical pulse transfers probability amplitude to the excited state. If the pulse has enough bandwidth, it excites several vibrational levels and generates a quantum wave packet that will then travel in a round trip across the excited-state potential surface, with certain group and phase velocities. The interaction with the second, delayed optical pulse generates an additional wave packet in the excited state. Enhancement or suppression of the excitation probability arises from constructive or destructive quantum interference, respectively, between these two wave packets. Alternatively, the results can be interpreted in the frequency domain, where the time delay between the phase-locked pulses translates into a modulation of the spectrum.

Averaging the response of 52 investigated molecules returns the ensemble oscillation in excitation probability as a function of Δt (Fig. 2c). In spite of its smaller amplitude in comparison to single molecules, the ensemble oscillation is clearly visible owing to the higher signal to noise ratio, and shows a good agreement with theoretical WPI calculations based on the bulk absorption spectrum (Fig. 2c).

In order to quantify the differences in ultrafast single-molecule responses, we performed a Fourier analysis of the fluorescence intensity versus Δt traces for 52 single molecules, and determined the main frequency component (f) and its corresponding phase (θ) (Fig. 2d). The frequencies range from roughly 20 to 45 THz (670 to 1,500 cm^{-1}), with a sharp peak around 32 THz (1,070 cm^{-1}), and are consistent with the energies of the vibrational bands observed for this molecule in bulk[29]. The distribution of frequencies reflects underlying variations in the energy and relative intensities of the vibrations for individual molecules. Analogous variations in the emission spectrum of single molecules have been ascribed to the influence of different local environments, in the form of varying dispersive interactions and structural constraints imposed by the polymer matrix[30].

The broader distribution of phases indicates variations in the electronic excitation energy of the molecules. Phases ranging from 0 to 2π are found, but the distribution is not uniform; it features a small peak, which causes the contrast in the ensemble fluorescence oscillation. This experiment already shows that the observation of ultrafast dynamics at the single-molecule level is feasible, and demonstrates its potential to discriminate between individual and ensemble-averaged responses.

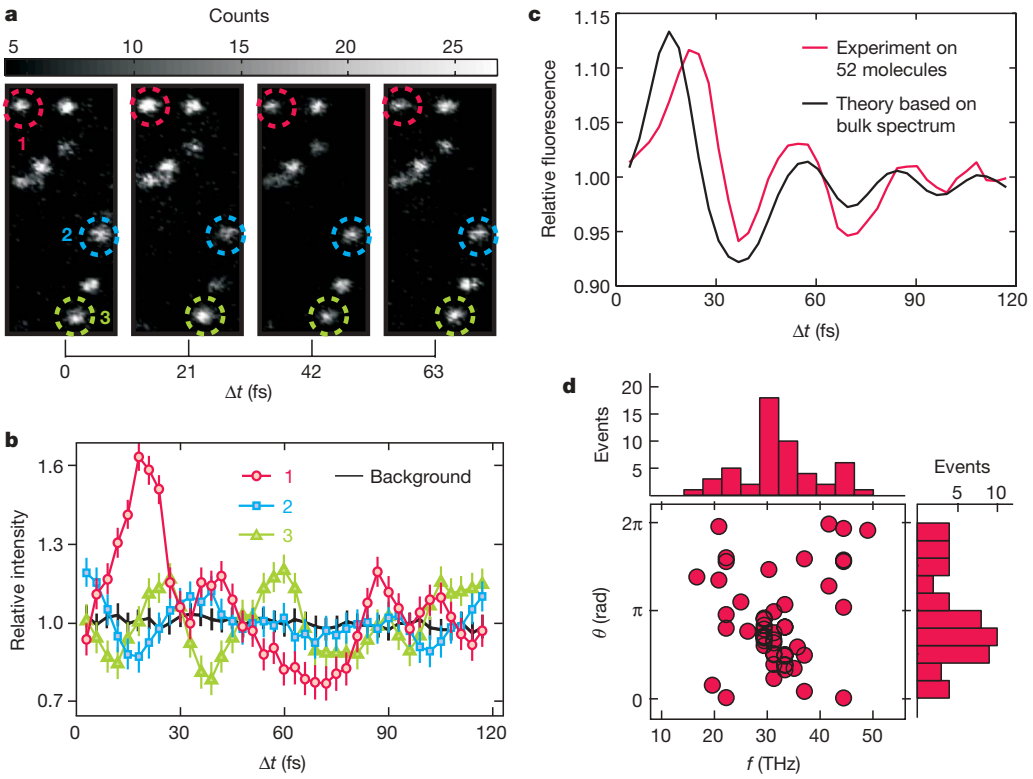

Figure 2 | Single-molecule wave-packet interference. **a**, Fluorescence images of single molecules excited with two mutually delayed (Δt), phase-locked laser pulses. **b**, Integrated intensity as a function of Δt for the fluorescence emission of the three molecules marked in **a**. A typical background trace is shown for reference. The traces are normalized to their respective average in order to visualize fluctuations in the intensity. Error bars, ± 1 s.d. **c**, Averaged response of 52 molecules compared to the theoretical prediction based on the bulk absorption spectrum. **d**, Result of the Fourier analysis of 52 single-molecule traces. Distributions and scatter plot of the main frequency component (f) and its corresponding phase (θ). Marker size and bin width include the experimental errors.

One of the most important features of WPI is that the phase of the generated wave packet is determined by both the vibrational levels involved and the phase of the optical field. This interdependence of the optical and wave-packet phases is the basis for the coherent control of molecular states. A clear-cut experiment to target the phase dependence of WPI is a time-delayed two-pulse excitation scheme, where the pulses have a mutual phase shift of π (ref. 28). We recorded the fluorescence of single molecules at each time delay Δt consecutively with the two pulses in phase ($\phi = 0$) and antiphase ($\phi = \pi$). Two examples are shown in Fig. 3a and b. Excitation with two pulses in phase, or with two pulses in antiphase, produces an inverted molecular response, in agreement with the expected inverse wave-packet interferences. This is confirmed by fits based on the bulk absorption spectrum (Fig. 3a).

For some molecules with high photostability, we could detect WPI in the excitation probability for times as long as 120 fs, showing fluctuations that are more complex than a damped, single frequency oscillation (Fig. 3b). In order to explore this complexity and investigate the limits of the fluorescence excitation enhancement and suppression achievable on a single molecule, we designed a multiple-pulse coherent excitation experiment. The idea is straightforward: as a wave packet propagates, its internal phase evolves with a certain phase velocity that depends on the amplitudes and phases of the vibrational states that are superimposed to form the wave packet. If one aims for maximum interference between two wave packets generated with a time delay Δt, a certain phase shift should be introduced in the second wave packet to compensate for the phase evolution of the first one. The resulting wave packet can then be made to interfere with subsequently launched wave packets to optimize state preparation. We used a train of four phase-locked pulses and varied Δt and ϕ independently. In this way, for each individual molecule, we obtained a time–phase map of the photoexcitation probability that provides a direct view into the molecular coherent dynamics.

We mapped the excitation probability as a function of (Δt, ϕ) for a large number of molecules, and found a rich variety of coherent dynamics. Four examples are shown in Fig. 4a–d. The influence of phase on the photoexcitation probability is evident. For any given delay, the opposite behaviour is observed for a phase shift of π. Diagonal bands of enhanced or suppressed photoexcitation probability can be seen. These are indications of the time–phase relation and clearly show how the wave-packet phase evolution can be followed by the optical field. The maximum enhancement or reduction of the excitation probability occurs for different combinations of delay and phase shift, depending on the molecule. When the excitation field is tailored to match the coherent dynamics of each molecule in its particular local environment, remarkably high degrees of control are achieved. Depending on the molecule, the control contrast (defined as the ratio of maximum to minimum excitation probability) ranges from 2.5 to as high as 4, which is approximately double that obtained with two pulses in phase or in antiphase (Fig. 2b and 3) and up to 3 times higher than the contrast we measured in bulk (Fig. 2c).

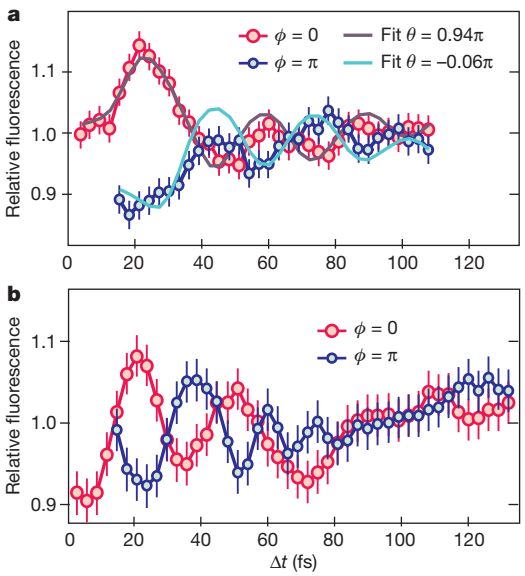

Figure 3 | Phase control of single-molecule wave packets. Single-molecule fluorescence intensity as a function of the time delay between two in-phase ($\phi = 0$) and in-antiphase ($\phi = \pi$) excitation pulses. The excitation intensity was constant for all (Δt, ϕ) combinations except for the (excluded) points near zero delay with $\phi = \pi$. **a**, The fits to the ($\phi = 0$) and ($\phi = \pi$) traces are based on the bulk absorption spectrum. Fourier analysis of the fits shows that $f = 31$ THz in both traces and the difference in θ is π. **b**, Some molecules present fluctuations even for time delays Δt as long as 120 fs and with more than one frequency component. Error bars, ± 1 s.d.

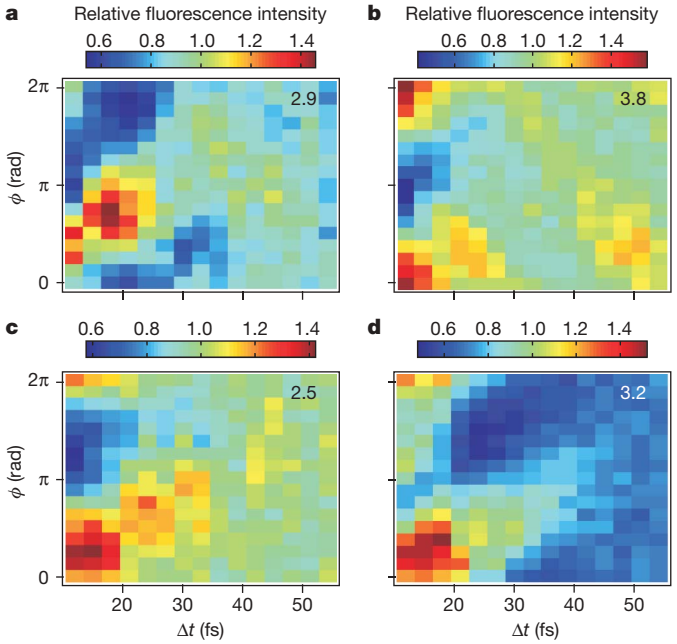

Figure 4 | Single-molecule time-phase coherent excitation maps. **a–d**, Time-phase fluorescence excitation maps of four different molecules excited with a four-pulse sequence. Δt and ϕ are the time delay and phase shift between each consecutive pulse in the sequence. The fluorescence intensity (colour scale) is normalized to the average. The maximum/minimum ratio, that is, the contrast achievable through control of coherent excitation, is shown in the upper right corner of each plot.

These experiments merge two of the most valuable experimental techniques of the past decades: ultrafast spectroscopy and single-molecule detection. They demonstrate that room-temperature coherent control experiments in ensembles are limited by intrinsic inhomogeneities, and at the same time provide the ultimate solution. The coherent dynamics of each molecule can be mapped at ambient conditions, and the excitation field can be tailored to obtain maximum control. We believe that this greatly extends the field of application and the potential of coherent control. Investigations addressing coherent dynamics and energy flow in complex systems and environments are among the possibilities. Examples include light-harvesting complexes, photo-active proteins, conjugated polymers and metallic or metal–organic hybrid nanostructures. Furthermore, single-molecule detection offers the possibility of multi-parameter correlations, such as the relation between molecular conformation and function.

METHODS SUMMARY

The highly photostable chromophore dinaphtoquaterrylenebis(dicarboximide) (DNQDI)[29] was embedded in thin polymer films in concentrations sufficiently low to allow individual DNQDI molecules to be spatially resolved in an epi-fluorescence confocal microscope, where they were excited with a sequence of up

to four phase-locked laser pulses. A femtosecond laser system combined with a pulse shaper was used to generate the excitation pulses with controllable inter-pulse delays and phase shifts. The excitation intensity was kept low enough to ensure a linear relationship between the fluorescence intensity and the excitation probability. The repetition rate of the laser system was high enough to enable the detection of single-molecule fluorescence and sufficiently low to accommodate the fluorescence lifetime of DNQDI between successive trains of excitation pulses. Further experimental details can be found in the Methods.

Full Methods and any associated references are available in the online version of the paper at www.nature.com/nature.

Received 24 November 2009; accepted 20 April 2010.

1. Rabitz, H. *et al.* Whither the future of controlling quantum phenomena? *Science* **288,** 824–828 (2000).
2. Bandrauk, A. D., Fujimura, Y. & Gordon, R. J. *Laser Control and Manipulation of Molecules* (Oxford Univ. Press, 2002).
3. Dantus, M. & Lozovoy, V. V. Experimental coherent laser control of physicochemical processes. *Chem. Rev.* **104,** 1813–1859 (2004).
4. Herek, J. L. *et al.* Quantum control of energy flow in light harvesting. *Nature* **417,** 533–535 (2002).
5. Engel, G. S. *et al.* Evidence for wavelike energy transfer through quantum coherence in photosynthetic systems. *Nature* **446,** 782–786 (2007).
6. Prokhorenko, V. I. *et al.* Coherent control of retinal isomerization in bacteriorhodopsin. *Science* **313,** 1257–1261 (2006).
7. Kuroda, D. G. *et al.* Mapping excited-state dynamics by coherent control of a dendrimer's photoemission efficiency. *Science* **326,** 263–267 (2009).
8. Zewail, A. H. Femtochemistry: atomic-scale dynamics of the chemical bond. *J. Phys. Chem. A* **104,** 5660–5694 (2000).
9. Basche, T. *et al. Single-Molecule Optical Detection, Imaging and Spectroscopy* (VCH, 1996).
10. Moerner, W. E. A dozen years of single-molecule spectroscopy in physics, chemistry, and biophysics. *J. Phys. Chem. B* **106,** 910–927 (2002).
11. Michalet, X., Weiss, S. & Jäger, M. Single-molecule fluorescence studies of protein folding and conformational dynamics. *Chem. Rev.* **106,** 1785–1813 (2006).
12. Lu, H. P., Xun, L. & Xie, X. S. Single-molecule enzymatic dynamics. *Science* **282,** 1877–1882 (1998).
13. Yildiz, A. *et al.* Myosin V walks hand-over-hand: single fluorophore imaging with 1.5-nm localization. *Science* **300,** 2061–2065 (2003).
14. Elf, J., Li, G. & Xie, X. S. Probing transcription factor dynamics at the single-molecule level in a living cell. *Science* **316,** 1191–1194 (2007).
15. Zondervan, R. *et al.* Local viscosity of supercooled glycerol near T_g probed by rotational diffusion of ensembles and single dye molecules. *Proc. Natl Acad. Sci. USA* **104,** 12628–12633 (2007).
16. Barbara, P. F. *et al.* Single-molecule spectroscopy of conjugated polymers. *Acc. Chem. Res.* **38,** 602–610 (2005).
17. Gerhardt, I. *et al.* Coherent state preparation and observation of Rabi oscillations in a single molecule. *Phys. Rev. A* **79,** 011402 (2009).
18. Van Dijk, E. M. H. P. *et al.* Single-molecule pump-probe detection resolves ultrafast pathways in individual and coupled quantum systems. *Phys. Rev. Lett.* **94,** 078302 (2005).
19. Shapiro, M. & Brumer, P. Coherent control of molecular dynamics. *Rep. Prog. Phys.* **66,** 859–942 (2003).
20. Judson, R. & Rabitz, H. Teaching lasers to control molecules. *Phys. Rev. Lett.* **68,** 1500–1503 (1992).
21. Assion, A. *et al.* Control of chemical reactions by feedback-optimized phase-shaped femtosecond laser pulses. *Science* **282,** 919–922 (1998).
22. Levis, R. J., Menkir, G. M. & Rabitz, H. Selective bond dissociation and rearrangement with optimally tailored, strong-field laser pulses. *Science* **292,** 709–713 (2001).
23. Bardeen, C. J. *et al.* Feedback quantum control of molecular electronic population transfer. *Chem. Phys. Lett.* **280,** 151–158 (1997).
24. Dudovich, N., Oron, D. & Silberberg, Y. Single-pulse coherently controlled nonlinear Raman spectroscopy and microscopy. *Nature* **418,** 512–514 (2002).
25. Bartels, R. *et al.* Shaped-pulse optimization of coherent emission of high-harmonic soft X-rays. *Nature* **406,** 164–166 (2000).
26. Amstrup, B. *et al.* The use of pulse shaping to control the photodissociation of a diatomic molecule: preventing the best from being the enemy of the good. *J. Phys. Chem.* **95,** 8019–8027 (1991).
27. Hornung, T., Motzkus, M. & De Vivie-Riedle, R. Teaching optimal control theory to distil robust pulses even under experimental constraints. *Phys. Rev. A* **65,** 021403 (2002).
28. Scherer, N. F. *et al.* Fluorescence-detected wave packet interferometry: time resolved molecular spectroscopy with sequences of femtosecond phase-locked pulses. *J. Chem. Phys.* **95,** 1487–1511 (1991).
29. Avlasevich, Y. S. *et al.* Novel core-expanded rylenebis(dicarboximide) dyes bearing pentacene units: facile synthesis and photophysical properties. *Chem. Eur. J.* **13,** 6555–6561 (2007).
30. Macklin, J. J. *et al.* Imaging and time-resolved spectroscopy of single molecules. *Science* **272,** 255–258 (1996).

Acknowledgements We thank P. Fendel from Menlo Systems for lending us an Octavius system and for technical assistance. We are grateful to Biophotonic Solutions Inc. for collaborating with us in developing the double-pass pulse shaper. We appreciate discussions with A. G. Curto and M. Castro López. This work was supported by the 'Molecular walker' project of the Koerber foundation (Hamburg) and by the Spanish Ministry of Science and Innovation (CSD2007-046-NanoLight.es and MAT2006-08184).

Author Contributions D.B., F.D.S. and N.F.v.H. conceived and designed the experiments. D.B., F.K. and R.H. constructed the experimental set-up. D.B. and F.D.S. carried out the measurements and analysis. D.B., F.D.S. and T.H.T. performed control experiments. Y.A. and K.M. provided the fluorescent molecules. F.D.S., D.B. and N.F.v.H. wrote the manuscript.

Author Information Reprints and permissions information is available at www.nature.com/reprints. The authors declare no competing financial interests. Readers are welcome to comment on the online version of this article at www.nature.com/nature. Correspondence and requests for materials should be addressed to F.D.S. (Fernando.Stefani@df.uba.ar) or N.F.v.H. (Niek.vanHulst@ICFO.es).

METHODS

Experimental set-up. A broad-band, temperature and atmosphere (100% N_2 with 0.05 bar overpressure) stabilized, Ti:sapphire oscillator (Octavius 85M, Menlo Systems) was used to obtain femtosecond pulses in the visible–near-infrared at a repetition rate of 85 MHz. For the molecular excitation, a band of 120 nm, centred at 676 nm, was selected and compressed to 15-fs pulses in the focus of a 1.3 NA Zeiss Fluar objective. Pulse shaping was performed with a double-pass 4f-shaper based on a liquid crystal spatial light modulator (Biophotonic Solutions). After spatial filtering, pulse characterization was carried out at the sample plane using the multiphoton intrapulse interference phase scan (MIIPS) method. The fluorescence of single molecules was detected in an epi-fluorescence confocal configuration. Suitable optical filters were used to separate the Stokes shifted fluorescence emission from residual excitation light, which was suppressed to a fraction of about 10^{-10} in the detected signals from single molecules. Avalanche photo-diodes (APDs, Perkin-Elmer) were used as single photon detectors. The photon collection-and-detection efficiency of the set-up was 2%.

Sample preparation. Dinaphtoquaterrylenebis(dicarboximide) (DNQDI; N,N′-bis-(N-2,6-diisopropylphenyl)-1,6,11,16-tetrakis[4-(1,1,3,3-tetramethylbutyl)-phenoxy]-8,9:18,19-dinaphthoquaterrylene-3,4:13,14-bis(dicarboximide))[29] molecules were immobilized in a poly(methyl-methacrylate) film spin-cast from a toluene solution onto a standard microscopy glass coverslip. Conditions were adjusted to obtain a film thickness of about 40 nm and one DNQDI molecule per square micrometre on average. DNQDI has a fluorescence lifetime of about 3 ns, a quantum efficiency of 40% and a molar extinction coefficient $\varepsilon = 142{,}900\,M^{-1}\,cm^{-1}$ ($62{,}800\,M^{-1}\,cm^{-1}$) at 700 nm (638 nm)[29].

Measurement procedures. Images (Fig. 2) were obtained by scanning a $10 \times 10\,\mu m^2$ area of the sample on a 256×256 pixel grid with an integration time of 6 ms per pixel. Fluorescence versus Δt traces (Figs 2 and 3) were obtained by selecting a region of interest (ROI) containing the image of one molecule and integrating the fluorescence of all pixels in that ROI. The $(\Delta t, \phi)$ excitation maps (Fig. 4) were obtained by monitoring the fluorescence emission of the single molecules for 400 ms at each combination of $(\Delta t, \phi)$. In between different $(\Delta t, \phi)$ combinations, the excitation light was blocked for another 400 ms (as shown in Fig. 1b). The series of $(\Delta t, \phi)$ values was repeated until the molecule photobleached. Only molecules for which each $(\Delta t, \phi)$ combination could be measured at least twice were considered. Owing to the fixed acquisition time, the shot-noise level varies; typically, each data point was determined with a total of 4,000 photons which gives a shot-noise level of 1.5%. For the measurements shown in Fig. 2, the laser power fluctuations were determined to be $<5\%$ and for the measurements in Figs 3 and 4, $<2\%$. Thus, the total uncertainty of the data ranges from 2.5% to 6%. The 85 MHz repetition rate of the laser system was high enough to enable the detection of single-molecule fluorescence and sufficiently low to accommodate the fluorescence lifetime of DNQDI between successive trains of excitation pulses. The excitation power was 1×10^{-5} W (1.2×10^{-14} J per pulse) in all measurements, which corresponds to roughly 1/80 of the intensity needed for fluorescence saturation and gives typical detected single-molecule count rates of $(3–4) \times 10^3$ counts s^{-1} with a signal-to-background ratio SBR ≈ 10 for the integrated signals. For the measurements shown in the paper, single-molecule fluorescence count rates (in units of 10^3 counts s^{-1}) are as follows. Fig. 2b; 4.1 for trace 1, 3.3 for trace 2, 3.6 for trace 3; Fig. 3a, 6.0; Fig. 3b, 3.8; Fig. 4a, 4.1; Fig. 4b, 3.1; Fig. 4c, 3.8; Fig. 4d, 5.2. Background count rates (in units of counts s^{-1}): Fig. 2, 300; Fig. 3, 400; Fig. 4, 300; of the background, 130 counts s^{-1} (that is, ~40%) consists of detector dark counts.